1.0

4.5
5.0
5.6

2.8

2.5

1.1

3.2
3.6

4.0

2.2

2.0

1.8

1.25

1.4

1.6

A Review of the Air Chemistry and
Relevant Parameters for the Modelling of the
Nuclear Induced Lightning

A. W. ALI

Plasma Physics Division

May 31, 1984

AD-A142 818

DTIC
ELECTE
JUL 5 1984

B

NAVAL RESEARCH LABORATORY
Washington, D.C.

84 07 03 089

REPORT DOCUMENTATION PAGE

1a REPORT SECURITY CLASSIFICATION UNCLASSIFIED		1b RESTRICTIVE MARKINGS			
2a SECURITY CLASSIFICATION AUTHORITY		3 DISTRIBUTION AVAILABILITY OF REPORT Approved for public release; distribution unlimited.			
2b DECLASSIFICATION DOWNGRADING SCHEDULE					
4 PERFORMING ORGANIZATION REPORT NUMBER(S) NRL Memorandum Report 5341		5 MONITORING ORGANIZATION REPORT NUMBER(S)			
6a NAME OF PERFORMING ORGANIZATION Naval Research Laboratory	6b OFFICE SYMBOL (If applicable) Code 4700.1	7a NAME OF MONITORING ORGANIZATION			
6c ADDRESS (City State and ZIP Code) Washington, DC 20375		7b ADDRESS (City State and ZIP Code)			
8a NAME OF FUNDING/SPONSORING ORGANIZATION Defense Nuclear Agency	8b OFFICE SYMBOL (If applicable)	9 PROCUREMENT INSTRUMENT IDENTIFICATION NUMBER MIPR No. 83-659 and 84-601			
8c ADDRESS (City State and ZIP Code) Washington, DC 20305		10 SOURCE OF FUNDING NOS			

		PROGRAM ELEMENT NO	PROJECT NO.	TASK NO	WORK UNIT NO
Washington, DC 20305		62715H			47-1924-04
11 TITLE (Include Security Classification) (See page ii)					

12 PERSONAL AUTHOR(S) A. W. Ali				
13a TYPE OF REPORT Interim	13b TIME COVERED FROM 4/83 TO 10/83	14 DATE OF REPORT (Yr., Mo., Day) May 31, 1984		15 PAGE COUNT 50
16 SUPPLEMENTARY NOTATION (See page ii)				

17	COSATI CODES		18 SUBJECT TERMS (Continue on reverse if necessary and identify by block number)
FIELD	GROUP	SUB GR	Air chemistry Attachment
			Reaction rates Recombination

19 ABSTRACT (Continue on reverse if necessary and identify by block number)

A review of the relevant processes for the modelling of NIL and their rate coefficients is given. These include the attachment rates, the ionization frequency, the electron temperature, the various recombinations and thermal processes.

20 DISTRIBUTION AVAILABILITY OF ABSTRACT UNCLASSIFIED UNLIMITED X SAME AS RPT ☐ DTIC USERS ☐	21 ABSTRACT SECURITY CLASSIFICATION UNCLASSIFIED	
22a NAME OF RESPONSIBLE INDIVIDUAL A. W. Ali	22b TELEPHONE NUMBER (Include Area Code) (202) 767-3762	22c OFFICE SYMBOL Code 4700.1

DD FORM 1473, 83 APR   EDITION OF 1 JAN 73 IS OBSOLETE

11. TITLE (Include Security Classification)

A REVIEW OF THE AIR CHEMISTRY AND RELEVANT PARAMETERS FOR THE MODELLING OF THE NUCLEAR INDUCED LIGHTNING

16. SUPPLEMENTARY NOTATION

<div align="center">CONTENTS</div>

DTIC
ELECTE
JUL 5 1984
S   D
B

Accession For

NTIS GRA&I
DTIC TAB   ☐
Unannounced   ☐
Justification _____

By_____
Distribution/ _____
Availability Codes

Dist | Avail and/or
      | Special

A-1

SYNOPSIS

To model the nuclear induced lightning, the basic processes responsible for this phenomenon must be understood. The air chemistry plays an essential role in such a modelling. However, a self consistent approach to the modelling requires the incorporation of the best available reaction rates and cross sections for the basic processes. A review of these processes and the relevant rates is undertaken for the sake of a realistic modelling of NIL.

A REVIEW OF THE AIR CHEMISTRY AND RELEVANT PARAMETERS FOR THE MODELLING OF THE NUCLEAR INDUCED LIGHTNING

1. INTRODUCTION

Nuclear induced lightning (NIL) has been observed[1] from detonations at the sea level (sunface bursts). These discharges occur some distance away (900 - 1400 meters) from the burst point and they grow, from the top of structures which are above ground by some meters, upwards to the cloud level. The growth velocity of the discharge is found[1] to be $\sim 1 - 2 \times 10^7$ cm/sec and that the discharge luminosity lasts for times of ~ 0.1 sec.

The mechanism for the discharge propagation, i.e., the streamer initiation and propagation, requires the presence of charges and electric fields. These physical quantities arise from the interaction of γ -rays, produced by the nuclear detonation, with the air molecules. The interaction produces Compton electrons which move outward, ionizing air species in its path, resulting in a plasma current moving in the opposite direction. These processes are understood to generate, the charges and electric fields which are responsible for the discharge initiation near sharp objects. A simple and semi-quantitative analysis for the electric field has been performed in Ref. 1, where the the radial electric field is estimated to be 300 Vcm^{-1}. This value for the field is much below the air breakdown threshold field[2] of 30 Vcm^{-1} $Torr^{-1}$.

The NIL phenomenon is complex and requires a multidisciplinary approach for its understanding and modelling. The modelling should comprise the following areas of physics and chemistry: interaction of radiation with air species, ionization of air and generation of air conductivity, electromagnetic equations to solve for the electric field in conjunction with the

conductivity, the air chemistry, air heating, hydrodynamic and flow equations, breakdown, streamer propagation, and discharge radiation.

A comprehensive modelling of NIL in time and space, which encompasses all physics aspects discussed above, is an approach which could lead to a complete understanding of the phenomenon, even though such an approach may be an ambitious one. A step in this direction has been undertaken by Longmire, et al[3]. The success of the modelling of NIL or any other phenomenon, however, depneds on a large measure on the assumptions made, the availability and accuracy of the relevant data used for the basic processes involved. For nuclear induced lightning the air chemistry plays an important role. This role is apparent in two important areas of the lightning discharge. The first, clearly is exhibited in the γ -ray generated conductivity in the disturbed region of the atmosphere, and the other is the air chemistry at the tip of the sharp object from which the streamer propagates.

This report deals with the air chemistry relevant to NIL, where it reviews the rate coefficients for the apporpriate processes and provides current and best values for modelling purposes. Various atmospheric models exists for EMP calculations and a study[4] has been made to determine the uncertainties in these calculations due to various chemistry models and coefficients. Scheibe[5] have considered the generation of smog! and its role in the electron attachment in an EMP environment at the sea level. Grover and Gilmore[6] have reviewed the mobility and attachment data for the EMP environment.

An important element in the NIL modelling is the air conductivity whose calculation depends heavily on the air chemistry. The conductivity is a function of the electron density, and ion density when the conductivity is due to ions, and their collision frequencies with the neutral species. The electron and ion density calculations require a set of rate equations which

determine their production and loss mechanisms. These processes are numerous and involve a large number of reaction and their coefficients which are temperature dependent. The collision frequency, on the other hand, can be obtained if the appropriate velocity distributions are known along with the relevant cross sections. This approach requires one to solve the Boltzmann equation. Other approaches are also available, e.g. assuming a Maxwellian velocity distribution for the electrons, or utilizing the appropriate particle mobilities obtained experimentally as a function of E/p and the average electron energies, also obtained experimentally as a function of E/p. The air chemistry near the tip requires a detailed treatment of air heating processes and the energy flow into various modes of freedom, e.g. kinetic, vibrational, etc. as well as the ionization frequency as a function of E/p.

This report deals with the prospect of a comprehensive NIL modelling and tries to provide the basic data for the most important processes. These processes are: attachment, ion-ion recombination, ionization frequency, association reactions, dissociative recombination, vibrational excitation and relaxation, the electron temperature, thermal processes and others.

2. ATTACHMENT

The electron attachment to O_2 in air proceeds mainly by the following processes

$$e + O_2 \rightarrow O^- + O \tag{1}$$

$$e + O_2 + M \rightarrow O_2^- + M \tag{2}$$

3

The first process, the dissociative attachment, has a threshold of ~ 4.3 eV and hence it is important when the electron energy is high. The cross section[7] for the dissociative attachment has been averaged[8] with the electron velocity over a Maxwellian electron velocity distribution and the corresponding rate coefficient is given in Table 1 as a function of the electron temperature.

Table I The Dissociative Attachment Rate Coefficient for O_2

$T_e(eV)$	Rate Coefficient(cm^3/sec)	$T_e(eV)$	Rate
0.1	6.42(-30)	2.6	2.57(-11)
0.2	1.89(-20)	2.7	2.67(-11)
0.3	3.61(-17)	2.8	2.76(-11)
0.4	1.78(-15)	2.9	2.84(-11)
0.5	1.93(-14)	3.0	2.91(-11)
0.6	9.58(-14)	3.1	2.97(-11)
0.7	3.0 (-13)	3.2	3.03(-11)
0.8	7.0 (-13)	3.3	3.08(-11)
0.9	1.35(-12)	3.4	3.12(-11)
1.0	2.25(-12)	3.5	3.15(-11)
1.1	3.4 (-12)	3.6	3.19(-11)
1.2	4.76(-12)	3.7	3.21(-11)
1.3	6.28(-12)	3.8	3.24(-11)
1.4	7.93(-12)	3.9	3.25(-11)
1.5	9.65(-12)	4.0	3.27(-11)
1.6	1.14(-11)	4.1	3.28(-11)
1.7	1.31(-11)	4.2	3.29(-11)
1.8	1.48(-11)	4.3	3.29(-11)
1.9	1.65(-11)	4.4	3.30(-11)
2.0	1.81(-11)	4.5	3.29(-11)
2.1	1.96(-11)	4.6	3.29(-11)
2.2	2.10(-11)	4.7	3.29(-11)
2.3	2.35(-11)	4.8	3.28(-11)
2.4	2.36(-11)	4.9	3.27(-11)
2.5	2.47(-11)	5.0	3.26(-11)

The data of Table I, however, can be expressed (within 20%) and in the temperature range of (0-5) eV by the following expression

$$a_2 = 1.0 \times 10^{-11} [2.28 + 11.6 \ T_e - 1.75 \ T_e^2] \ T_e^{-0.5} \ Exp(-4.2/T_e) \qquad (3)$$

Where T_e is in units of eV.

The three-body attachment process as given by Eq. 2 indicates that M is the third body which may be O_2, N_2, H_2O, CO_2 and any other molecular compound generated in the disturbed air.

Considerable measurements on the three-body attachment rate coefficient exists, indicating the predominance of this attachment for electrons with energy[9] of < 1.0 eV . The Measurements, prior to 1971, have been reviewed by Phelps[9,10] and recommended rate coefficients for attachment to O_2 are given for various third bodies appearing in Eq. 2. These and more recent measurements which are reviewed here, have been performed for thermal electrons and over a limited range of E/p. And are mainly obtained from swarm and electron beam experiments.

2.1 THREE BODY ATTACHMENT (M=O_2)

For the three body attachment in pure O_2 and for thermal electrons at 300°K, the measured values of various workers are in good agreement. These values, in units of cm^6/sec, are: $(2.8 \pm 0.5) \times 10^{-30}$ [Ref. 11], 2.0×10^{-30} [Ref.12], $(2.4 \pm 0.1) \times 10^{-30}$ [Ref. 13 and 14], $(2.1 \pm 0.2) \times 10^{-30}$ [Ref. 15], 3.8×10^{-30} [Ref. 16], 2.1×10^{-30} [Ref. 17], ~ 2.5×10^{-30} [Ref. 18]. It seems that a value of 2.4×10^{-30} cm^6/sec is a resonable value for thermal electrons at gas temperature of 300°K. The temperature dependence of the

three-body rate coefficient, $a_3(O_2)$, where O_2 is the third body, have been obtained in swarm experiments from the attachment coefficients per unit length, η, which are measured[11,12,19] as a function of $\frac{E}{N}$ (or E/p) . In general, $a_3(O_2)$ is related to η according to (4)

$$\eta \, V_d = a_3(O_2) \, O_2^{2} \tag{4}$$

where V_d is the electron drift velocity which is a function of E/N (or E/p) and has been measured in a large number of gaseous media[20]. The attachment coefficient per unit length signifies the total attachment in O_2, i.e., the two-body and the three-body processes delineated experimentally where the two body is independent of pressure and important at high E/p, in contrast the three-body is pressure dependent and predominates in the regions of low E/p. These characteristics can be seen in Figure 1 which is based on data from Reference 19.

The three-body attachment rate coefficient, $a_3(O_2)$ can be obtained from data such as the one given in Figure 1, Equation 3 and the drift velocity as a function of E/p. In addition one needs the data for the mean electron energy or the characteristic energy ($\sim T_e$) which are also measured as a function of E/p. From these considerations one obtains $a_3(O_2)$ as a function of T_e, where most of the data are basically for electron temperatures of 1eV and lower with the gas temperature at 300°K. However, several measurements have been made where the gas temperature, T_g, is varied. Such data are as follows: Chanin, et al[11] for T_g between 77°K and 370°K, Pack and Phelps[12] for T_g between 300°K and 575°K and Truby[15] for T_g between 113°K and 300°K. Phelps[10] recommends the

7

following expression for the three-body attachment for thermal electrons when the gas temperature is varied from 300°K to 600°k

$$a_3 \ (O_2) = (1.4 \pm 0.2) \times 10^{-29} \left(\frac{300}{T_g}\right) Exp \left(- \frac{600}{T_g}\right) \tag{5}$$

On the other hand, the measured rate coefficient of Truby[15] fits the following expression.

$$a_3 \ (O_2) = 4 \times 10^{-30} \ Exp \ (- \ 193/T_g) \tag{6}$$

However, eventhough the measurements of Truby[15] are for temperatures below 300, his expression (Eq. 6) can be used for higher temperatures (up to 600°K) where it differs in value by 10% from that of Phelps[10] (Eq. 5).

The attachment rate coefficients as a function of the electron temperature are shown in Figure 2 based on various swarm data. These data show a smooth variation of the coefficient with the electron temperature. However, the data from the electron beam experiment[18], also shown in Figure 2, show definite structures as a function of the electron temperature. The peaks of the structures occur at the positions of the vibrational levels of the O_2^- system. This compound (resonance) state decays by autodetachnment which accounts[18] for the vibrational cross section of O_2. However, this state can be stabilized in collisions with O_2 resulting in a stable O_2^-. The structures observed by Spence and Schulz[18] establish the validity of the assumption[21] that the three-body attachment is a two step process, i.e.,

$$e + O_2 \rightarrow (O_2^-)^* \qquad (7)$$

$$(O_2^-)^* + O_2 \rightarrow O_2^- + O_2 \qquad (8)$$

The structure in the rate coefficient has also been observed by McCorkle, et al[16] especially for electrons with temperature below 0.1 eV as shown in Figure 2.

2.2 THREE-BODY ATTACHMENT (M=N_2)

The attachment to O_2 with N_2 as the third body has been measured by many workers[11,13,14,16] where the room temperature values of a_3 (N_2) are: 5.6 x 10^{-32} cm^6/sec [Ref. 11], 1.5 x 10^{-31} [Ref. 16], and 8.5 x 10^{-32} [Refs. 13 and 14]. The last value falls almost midway between the other two measurements and hence may be used as an average value at room temperature. The most recent measurements[13,16] which are performed at high pressure (< 300 Torr) are higher than the swarm data which were performed at pressures much lower than 300 Torr. These recent measurements indicate that at higher pressures[13] the attachment rate data do not reflect the three-body process and that one has to also invoke a four-body process[13,16,22]. These processes (see Eqs. 9 and 10) follow those in Eqs. 7 and 8 where the excited negative ion $(O_2^-)^*$ is converted into a coumpound of the form $[O_2^{-*} - N_2]$ in collisions with N_2. This compound then is stablized through a collision with O_2 or N_2, resulting in a stable O_2^- :

$$(O_2^-)^* + N_2 \rightarrow [O_2^{-*} - N_2] \qquad (9)$$

9

$$[O_2^{-*} - N_2] + O_2 \rightarrow O_2^- + N_2 + O_2 \qquad (10a)$$

$$[O_2^{-*} - N_2] + N_2 \rightarrow O_2^- + N_2 + N_2 \qquad (10b)$$

The temperature dependence of $a_3(N_2)$ based on the data of References 11, 16 and 22 are shown in Fig. 2. McCorkle, et al[16] indicate that if they replot the data of Chanin, et al[11] by obtaining the mean energy from the know electron energy distribution in N_2, an excellent ageeement between such a plot and McCorkle et al[16] data is realized.

In the four-body process (see Eqs. 9 and 10), it is found[13] that O_2 is more effective than N_2 in stabilizing O_2^- . The room temperature values for the four body attachment rate coefficients where O_2 and N_2 are the fourth bodies are[7]:

$$\alpha_4 \ (O_2) = 1.0 \times 10^{-49} \ cm^9/sec \qquad (11)$$

$$\alpha_4 \ (N_2) = 6.6 \times 10^{-52} \ cm^9/sec \qquad (12)$$

These processes increase the three body attahcment in one atmosphere of air at room temperature by ~ 20%.

2.3. THREE-BODY ATTACHMENT (M=H_2O)

The three-body attachment to O_2 with H_2O as the third body has been measured[23,24] for electrons at room temperature. The coefficients for a_3 (H_2O) are: $(1.4 \pm 0.2) \times 10^{-29}$ cm^6/sec [Ref. 23] and $(1.4 \pm 0.5) \times 10^{-29}$ cm^6/sec [Ref. 24] which are in excellent agreement. However, no data exist for this attachment for electron temperature above 400°K.

2.4 THREE-BODY ATTACHMENT IN DRY AIR

The coefficients obtained experimentally for the three-body and four-body attachment rates to O_2 with the third-body being O_2 and N_2 can be utilized to obtain the attachment rate in air. However, direct meansurements of the attachment rate in air also exists and are reviewed in this section. The room temperature rate coefficient for the three body attachment in air, a_3 (air), is $(1.1 \pm 0.07) \times 10^{-31}$ cm^6/sec [Ref. 17] which is obtained in air like mixture ($4N_2:O_2$). The electron life time measurements[25] in air afterglow plasma for air pressures between 50 and 600 Torr yield the following expression (which may have an uncertainty of ∼ 30%)

$$\tau = \frac{6.4 \times 10^{-3}}{p^2} \tag{13}$$

where p is in Torr. Accordingly, the life time of thermal electrons in one atmosphere is 1.1×10^{-8} sec. Similar results have been obtained by Price and VanLint[26]. Relation (13) implies that total attachment in air at 760 Torr is 1.24×10^{-31} cm^6/sec. If we accept the average values of a_3 (O_2) and a_3 (N_2) as 2.4×10^{-30} cm^6/sec and 8.5×10^{-32} cm^6/sec, respectively, the three-body attachment rate coefficient in air will be 1.05×10^{-31} cm^6/sec. If one

11

adds ~ 20% increase due to four body effects one obtains a rate coefficient of 1.25×10^{-31} cm^6/sec which is in good agreement with the lifetime measurement[25] and is shown in Fig. 3.

The temperature dependence of the three-body attachment in air has been measured by Schneider and Brau[27] in the temperature range of 0.45 to 1.2 eV. These measurements are shown on Fig. 3 along with the calculated values from the data of Fig. 2 where

$$a_3 \ (air) = 0.04 \ a_3 \ (O_2) + 0.16 \ a_3 \ (N_2) \tag{14}$$

In this case we have utilized the data for N_2 by McCorkle, et al[16] which is in excellent agreement with the data of Chanin, et al[11], replotted as a function of the average electron energy[16]. As for O_2, the data of Chanin, et al[11] and McCorkle, et al[16] were treated separately and the results are shown on Fig. 3 as a function of the electron temperature. It is obvious from the figure that good agreement exists for the coefficients for $T_e < 0.1$. Above $T_e > 0.1$ the two sets differ by as much as a factor of 3. However, the set obtained from the data of McCorkel, et al[16] merges in a resonable manner with those high temperature measurements of Schneider and Brau[27]. It is possible that if the right energy scale is utilized for $a_3 \ (O_2)$ of Ref. 11 its data will be shifted towards lower temperature resulting in better agreement with the data of Ref. 16.

2.5   THREE-BODY ATTACHMENT IN WET AIR

There are no temperature depended measurements for the three-body attachment to O_2 with H_2O as the third body. The data[23,24] for thermal

electrons at 300°K are in good agreement with a value of 1.4 x 10^{-29} cm^6/sec. This value indicates that H_2O is 6 times more effective than O_2 as a third-body in stabilizing O_2^- . If we assume that the temperature dependence of attachment with H_2O as the third body is similar to that with O_2 as the third body, then the three-body attachment rate with H_2O as the third body should follow the data in Fig. 2 with an increase in magnitude by a factor of 6. This has been done and the results are shown in Fig. 4.

If we utilize the room temperature value of the three body attachment to O_2 with H_2O as the third body (1.4 x $10^{-29}cm^6$/sec) and 1.25 x 10^{-31} cm^6/sec in dry air we obtain attachment rate for moist air. We consider three values of 2%, 4% and 5% for H_2O in air and calculate the attachment rate in moist air. The results are shown in Fig. 5 along with the experimental results of VanLint and Price[28].

3.   THE ELECTRON TEMPERATURE

In Section 2 we discussed the attachment rates in dry and wet air. It is obvious that these rates are dependent on the electron temperature which has to be known as a function of E/p for a realistic modelling of nuclear induced lightning. The electron temperature, defined[12] in the swarm experiments as the characteristic energy is often obtained as a function of E/p by measuring D_t/μ . Where D_t is the diffusion coefficient transverse to the direction of the electric field and μ is the electron mobility. The electron temperature, T_e, in dry air has been measured by many investigators[29-33] for a wide range of E/p. These measurements compiled by Gallaher et al[34] are shown in Figures [6 a,b] where good agreement is apparent, whenever more than one measurement exists for a given range of E/p.   However, no measurement of T_e exists for E/p below 0.1 V-cm^{-1}-$Torr^{-1}$.   On the other hand, T_e has been measured and calcualted[35-40] in both N_2 and O_2 for values of E/p far below 0.1 V cm^{-1}

13

Torr^{-1}. For N_2 the data of Jory[38] and Crompton and Elford[36] are shown in Figure [6b] along with the theoretical values of Hake and Phelps[40] for T_e in O_2.

It is interesting to note that the electron temperature measurements of Crompton et al[32] in air fall between the T_e values in N_2 and O_2 except for the data at lowest end of E/p. Furthermore, the T_e values in N_2 and O_2 get closer as E/p gets lower converging to the thermal value as expected. Assuming that the diffusion coefficient D_t is the same in N_2 and O_2 one can utilize the data for T_e in N_2 and O_2 to obtain T_e in air. This we have done and the result is shown in Fig. [6b].

However, for most modelling purposes one is also interested in the electron tempeature in moist air. Unfortunately no such measurement exists. On the other hand, measurements and calculations of T_e in pure water vapor exists. This data is shown in Fig. [6a] for the sake of comparison with T_e in dry air and is obtained from the measurements of Parr and Moruzzi[41] and that of Wilson, et al[42] whose D_L/μ measurements agree well with the theoretical values of Lowke and Parker[39]. From this figure one sees that the electron temperature rises very rapidly for E/p between 15 and 30 V cm^{-1} Torr^{-1}. For E/p > 20 V cm^{-1} Torr^{-1} the electron temperature in H_2O is slightly higher than that in dry air. However, for $\frac{E}{P}$ < 10 V cm^{-1} Torr^{-1}, the electron temperature in H_2O is much lower than that in dry air. In this region ($\frac{E}{P}$ < 10 V cm^{-1} Torr^{-1}) the electron temperature in H_2O is thermal (i.e. ~ 300°k) while the electron temperature in dry air is much higher (see Fig. 6a). Between E/p = 1.0 to 10.0 V cm^{-1} Torr^{-1} the electron temperature in air is 12 to 40 times higher than that in water vapor. Therefore, in moist air, the electron temperature will be lower than in the case of dry air, in the E/p range just alluded to. If one assumes, for the sake of argument that

14

the diffusion coefficient in H_2O is the same as in dry air then for air with 2.5% of H_2O the average electron temperature will be lowered from 1.3 eV for dry air to 0.55 eV which implies that water vapor has a large influence on the electron temperature for $E/p < 10$ V cm^{-1} $Torr^{-1}$.

4. ION-ION RECOMBINATION

In air a variety of positive and negative ions are formed as a result of the ionization of air molecules and the subsequent chemical processes. The positive ions recombine with the free electrons and the negative ions. The reocmbinations of the positive and negative ions proceed through the two and three-body neutralization processes i.e.,

$$A^+ + B^- \rightarrow A + B \qquad (15)$$
$$A^+ + B^- + M \rightarrow A + B + M \qquad (16)$$

where A^+ and B^- denote atomic, molecular and cluster ions.

4.1 TWO BODY ION-ION RECOMBINATION (α_2)

The two body mutual neutralization of positive and negative ions has been measured by the SR1 group[43] using the merging beam technique. Most of these measurments were concerned with atomic and molecular systems of interest shown in TABLE II.

15

TABLE II: TWO BODY MUTUAL NEUTRALIZATION COEFFICIENT

In Units of $10^{-7} cm^3/sec$ (Ref. 43 & 46) and $10^{-8} cm^3/sec$ (Ref. 44 & 45)

Reaction	Ref. 43	Ref. 46	Ref. 44 & 45
$O^+ + O^-$	2.7 ± 1.3		
$N^+ + O^-$	2.6 ± 0.8		
$O_2^+ + O^-$	1.0 ± 0.4		
$O_2^+ + O_2^-$	4.2 ± 1.3	1.0 ± 0.1	
$N_2^+ + O_2^-$	1.6 ± 0.5		
$NO^+ + O_2^-$	5.8 ± 1.0		
$N_2^+ + NO_2^-$	1.3 ± 0.5		
$NO^+ + NO_2^-$	5.1 ± 1.5	1.75 ± 0.6	6.4 ± 0.7
$O_2^+ + NO_2^-$	4.1 ± 1.3		
$NO^+ + NO_3^-$	8.1 ± 2.3	0.34 ± 0.12	5.7 ± 0.6
$O_2^+ + NO_3^-$	1.3 ± 0.4		
$H_3O^+ (H_2O)_3 + NO_3^-$			5.5
$H_3O^+ (H_2O)_3 + NO_3^- + HNO_3$			5.7

However, the mutual neutralizaiton rate coefficient, at room temperature, given in Table II by the SRI group[43] are obtained by extrapolation. The actual measurements are at energies of 0.15 eV and higher. These measuremnts are fit to a theoretical form predicted by Landau-Zener theory[43], and extrapolated to thermal energies and a rate coefficient is obtained from the product of the relative velocity of the ions and the cross section for neutralization. However, the afterglow measurements of Smith et al[44] and Smith and Church[45], for the reactions of NO^+ with NO_2^- and NO_3^- , predict

neutralization values which are an order of magnitude smaller than those of Moseley et al[43]. Eisner and Hirsh[46] have also measured these two reactions and obtained $[1.75 \pm 0.6] \times 10^{-7}$ cm^3/sec and $(3.4 \pm 1.2) \times 10^{-8}$ cm^3/sec for the neutralization of NO^+ with NO_2^- and NO_3^-, respectively. These values are lower from those predicted by Moseley et al[43] by a factor of 3 and 30 for the corresponding neutralizations, respectively. The discrepancy may lie in the extrapolation methods of Ref. [43].

Smith and his colleagues[44,45] have measured the neutralization coefficients for more complex ions (hydrates), in addition to those discussed above. they find that NO_3^- ions and their clusters, regardless of the degree of clustering behave similarly, i.e., the mutual neutralization coefficients of these simple and complex ions are in the range of $(5-6) \times 10^{-8}$ cm^3/sec (see Table II). This value is in good agreement with the measurements of Ulwick[47] in the upper atmosphere (50 - 75 km) which give a value of 6.5×10^{-8} cm^3/sec.

The temperature dependence of the ion-ion neutralization coefficient has the form of $(T_g)^{-0.5}$ which is predicted theoritically[48,49], and hence it can be utilized to obtain the coefficients at temperatures other than at 300°K.

Theoretical calculations of the ion-ion neutralization coefficients have been carried out by Olsen[48] based on a semiemperical absorbing sphere model. The predicted values in the majority of the cases, presented in Table II, are always below the experimentally obtained ones. It is interesting to note that in the case of $NO^+ + NO_3^-$ calculated value is lower by a factor of 7. For atomic and molecular ions, however, experimental predictions are higher by a factor of 2 compared to the calculated values.

A middle ground, for modelling purposes is to use a value of $1.5 \times 10^{-7} \left(\frac{300}{T_g}\right)^{0.5}$ for all neutralization which involve an atomic and molecular ion. However, whenever a triatomic or heavier molecule is involved,

17

the measured value of 5×10^{-8} cm^3/sec should be utilized. This same value should also be utilized for complex ions (hydrated ions).

4.2 THREE BODY ION-ION RECOMBINATION (α_3)

The three body ion-ion recombination of various air species ions of interest have been measured by McGowan[50] at room temperature and 760 Torr. These measurements are performed in clean air where the possible positive and negative ions were, N_4^+, N_3^+, NO^+, O_4^+, O_2^-, O_4^-, NO_2^- .

The recombination rate coefficient varied from 2.28×10^{-6} cm^3/sec to 2.18×10^{-6}cm^3/sec which imply a third body rate coefficient of 8.5×10^{-26} cm^6/sec and 8.10×10^{-26} cm^6/sec, respectively. When air contained water vapor, the ion-ion recombination rate coefficient varied from 6.1×10^{-26} cm^6/sec to 5.3×10^{-26} cm^6/sec for a relative humidty of 38% and 32%, respectively.

The value of ion-ion recombination coefficient in one atmosphere of air, 2.2×10^{-6} cm^3/sec, obtained by McGowan[50] is in good agreement with that measured by Sayers[51]. However, a recent determination[52] of α_3 in dry air (1 atm, 300°k) gives a value of 5.0×10^{-7} cm^3/sec which is smaller by a factor of 4 compared to that measured by McGowan[50].

From the theoretical point of view, the first attempt to calculate α_3 was made by Thompson[53]. Thompson's theory predicts results in good agreement with experimental findings for pressures below one atmosphere. The success of this theory, however, is largely fortuitous[54] and various attempts have been made[53,54] to refine it. At higher pressures, on the other hand, Langevin's Theory[53] is more appropriate and has a simple expression for the recombination based on the ionic mobility. Thus

$$\alpha_3 = 4\pi e^2 \ (\mu^+ + \mu^-) \tag{17}$$

18

Using the mobility data[55] for air ions, one obtains $\alpha_3 = 4.7 \times 10^{-6}$ cm^3/sec at 1 atmosphere which is larger by a factor of 2 compared to the measurements of McGowan[50]

5. IONIZATION FREQUENCY

The ionization frequency in air, ν_i , as a function of E/p is another important parameter for the modelling of the nuclear induced lightning. The ionization frequency, in general, is obtained from the ionization coefficient (Townsend coefficient) α and the drift velocity V_d where

$$\nu_i = \alpha \, V_d \tag{18}$$

The ionization coefficient in air has been measured by many investigators[33,56-59] and for a wide range of E/p. These measurements, (Ref. 3, 56 to 59) are in reasonable agreement especially those which are for clean air[58-59]. The old measurements[56,57] are not reliable at low E/p since they were contaminated[20] with mercury which has low ionization potential. A best fit to the data of Reference (58) yields the following expressions[60] with an error of < 14%

$$\frac{\alpha}{p} = 8.34 \, \mathrm{Exp} \, (- \, 273.8/E/p) \qquad 120 > \frac{E}{p} > 54 \tag{19}$$

$$\frac{\alpha}{p} = 16.0 \, \mathrm{Exp} \, (- \, 359/E/p) \qquad 1000 > E/p > 120 \tag{20}$$

The drift velocity in air, on the other hand, can be expressed[60] as

19

$$V_d = 6.0 \times 10^6 + 2.5 \times 10^5 \ (E/p) \qquad 54 < E/p < 120 \qquad (21)$$

$$V_d = 3.38 \times 10^6 \ (E/p)^{1/2} \qquad 120 < E/p < 1000 \qquad (22)$$

These expressions are obtained[60] using the measured drift velocities in nitrogen and oxygen. The corresponding ionization frequency in air is

$$\frac{\nu_i}{p} = [6.0 \times 10^6 + 2.5 \times 10^5 \ (E/p)] \ 8.34 \ \text{Exp} \ (\frac{-\ 273.8}{E/p}) \qquad (23)$$
for $\qquad\qquad 54 < E/p < 120$

$$\frac{\nu_i}{p} = 54.08 \times 10^6 \ (E/p)^{1/2} \ \text{Exp}(\frac{-359}{E/p}) \qquad (24)$$
for $\qquad\qquad 120 < E/p < 1000$

For the region below $\frac{E}{p} = 50$ V cm^{-1} Torr^{-1} , the drift velocity[61,62] in air fits the following expression

$$V_d = 8.7 \times 10^5 \ (E/p)^{0.76} \qquad 30 < E/p < 50 \qquad (25)$$

to within 10% of the data. For E/p below 54 V cm^{-1} Torr^{-1}, the ionization

coefficient can be expressed as

$$\frac{\alpha}{p} = 12.0 \, \text{Exp} \left(\frac{- \, 273.8}{E/p} \right) \qquad 37 < \frac{E}{p} < 54 \qquad (26)$$

which fits the measured[59] data to better than 10%. Thus the ionization frequency in air for $E/p = 37 - 54$ V cm^{-1} Torr^{-1} is
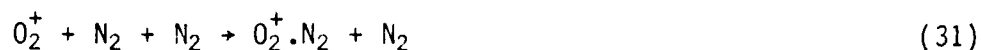
$$\frac{\nu_i}{p} = 1.04 \times 10^7 \, (E/p)^{0.76} \, \text{Exp} \left(\frac{- \, 273.8}{E/p} \right) \qquad (27)$$

This may be extended down to $\frac{E}{p} = 30$ V cm^{-1} Torr^{-1} which is the standard reduced breakdown field in air.

6. ASSOCIATION REACTIONS

In dry air the primary ions generated are N_2^+, O_2^+, N^+ and O^+ which undergo certain association reactions that convert them into heavier ions, e.g.,

$$N_2^+ + N_2 + N_2 \rightarrow N_4^+ + N_2 \qquad (28)$$

$$N^+ + N_2 + N_2 \rightarrow N_3^+ + N_2 \qquad (29)$$

$$O_2^+ + O_2 + O_2 \rightarrow O_4^+ + O_2 \qquad (30)$$

$$O_2^+ + N_2 + N_2 \rightarrow O_2^+ \cdot N_2 + N_2 \qquad (31)$$

$$NO^+ + N_2 + N_2 \rightarrow NO^+ \cdot N_2 + N_2 \qquad (32)$$

The dissociative recombinations of these air ion clusters with the plasma electrons proceed at a rapid rate compared to those of the light ions and hence affect drastically the plasma decay.

The association rate coefficient for reaction (28) has been measured[63-71] at room temperature and as a function of E/p where the most recent measurement[71] gives a value of 5.0×10^{-29} cm^6/sec. However, the dependence of this coefficient on the gas temperature has been investigated by Good, et al[68] in the temperature range of 300°k to 380°k and by Dheandhanoo, et al[71], in the temperature range of 120°k to 480°k. A temperature dependence of $T_g^{-4.0}$ can be inferred[72] from the measurement of Good et al[68], while the most recent measurement[71] gives a $T_g^{-2.2}$ dependence and it should be preferred since it is obtained over a wider range of T_g. Hence the most current rate coefficient for reaction (28) is $1.50 \times 10^{-32} (\frac{1}{T_g})^{2.2}$ cm^6/sec where T_g is in eV.

The coefficient for reaction (29) has been measured[68,69,71,73] and the room temperature value, in units of 10^{-29} cm^6/sec, is 2.7 [Ref 70], 5.0 [Ref 68], 1.8 [Ref 73] and 2.0 [Ref 71]. The most recent measurement[71] also provides the temperature dependence of the reaction which follows $(T_g)^{-2.0}$. Hence the most current coefficient for reaction (29) is $1.25 \times 10^{-32} (\frac{1}{T_g})^{2.0}$, with T_g in eV.

22

The coefficient for reaction (30) has been measured at room temperature[74,75] and as a function of the gas temperature[75,76] for the range of 80°k to 300°k (Ref. 75) and 300°k to 340°k (Ref. 76). The room temperature value is ~ 2.5 x 10^{-30} cm^6/sec and the temperature dependence varies as $T_g^{-2.8}$. Thus the rate coefficient for reaction (30) is $9 \times 10^{-35} (T_g)^{-2.8}$ where T_g is in eV.

As for reaction (31), its coefficient and temperature dependence, in a limited range, has been obtained most recently by Dheandhanoo, et al[71]. The coefficient is $7.5 \times 10^{-36} (T_g)^{-3.2}$ where T_g is in eV. However, for most modelling purposes one can ignore $O_2^+ \cdot N_2$, for two reasons. One, its collisional breakup with N_2 (~ 2 x 10^{-11} cm^3/sec)[76] is as rapid as its formation (in one atmosphere) and second is its rapid switching reaction[77] with O_2 leading to the formation of O_4^+.

The last reaction in this section for the dry air clusters (Eq. 32) has recently been meausred[71] and the coefficient is $2.68 \times 10^{-38} (T_g)^{-4.4}$ where T_g is in eV.

7. THERMAL PROCESSES

The streamer propagation is initiated near a sharp metallic tip which enhances the electric field. The ionization and heating of air in this region, which occurs as a result of ohmic heating, requires a detailed treatment of the air heating processes. The energy gained from the field by the electron is expended in collisions with the air molecules. These collisions are elastic and inelastic in nature and result in direct or indirect heating of the air species. The inelastic processes and their contribution to the heating of air molecules are

a) The Ionization Energy

Part of this energy returns into the gas through the dissociative

23

recombination of the molecular ions. If the ions are N_2^+ and O_2^+, the contributions per recombination to air heating are ~ 5.8 eV and 6.96 eV, respectively. On the other hand if these molecules are converted to N_4^+ and O_4^+ which is highly probable when the air is not heated at the beginning, then the contributrions per recombination to air heating are ~ 15.0 eV and 11.6 eV, respectively. This arises from the fact that the dissociative recombination of N_4^+ and O_4^+ result in excited N_2 and O_2 molecules which in turn are quenched by other molecules, resulting in heating of the air species.

b) Excitation of Electronic States

The energy lost by electrons in the excitation of the electronic states of N_2 and O_2, can be considered as indirect heating of the air species, because of their rapid quenching by N_2 and O_2. For example the $N_2(C,$ $v=o)$ state is quenched by N_2 and O_2 with a rate coefficient of $1.12 \times 10^{-11} cm^3/sec$ and $2.9 \times 10^{-10} cm^3/sec$. In one atmosphere of air, where most of our concern is, these coefficients imply that the (C, o) state is quenched with a rate of ~ $1.6 \times 10^9 sec^{-1}$ which is ~ 50 times faster than the radiative decay rate of the state. Hence, most of the energy lost by electron into the electronic states, of N_2, especially the triplets below 12 eV will be converted into the gas kinetic energy of the air molecules. However, the $A^3\Sigma$ state may result in the dissociation of O_2. For electronic states, higher than 12 eV, the most probable product is the dissociation[79] of the molecule. However, the electron energy loss to O_2 would result mainly in the dissociation of the molecule and the excitation of $a^1\Delta$ and $b^1\Sigma$ states which are metastable and are quenched in time scales much longer than ~ 1 m sec . However, they are destroyed by electron deexitation and by detachment of O_2^- . The rate of energy loss

to various states can be found in Ref. (60).

c). The Rotational and Vibrational Excitations

The electron energy loss to the rotational mode of the molecules is an inelastic process which indirectly heats the air moleucles. The rotational energy is rapidly converted into moleuclar kinetic energy. This is due to the fact that only few collisions are needed for the rotational energy relaxation into the thermal energy.

However, the electron energy loss into the vibrational mode generates an energy reservoir which does not return rapidly into the thermal mode. Therefore, it must be accounted separately with a detailed consideration for its coupling to the electron temperature and the gas kinetic temperature. This requires a master equation[80] for the vibrational level with electron excitation and dexcitations, vibrational-vibrational and vibrational-translational trasitions. The rate coefficients for the excitations of the first eight vibrational levels of N_2 is given in Table III. These coefficients are obtained[8,81] using the measured cross sections[82-84] averaged with electron velocity over an electron Maxwellian velocity distribution. The generation of excitation to higher levels, by electron impact, can be obtained from the following relation

$$X_{v, \, v+\Delta v} = X_{o, \, \Delta v} \tag{33}$$

The relaxation of the vibrational energy through heavy particle collisions i.e., the vibrational-translational transitions, mainly occur in collision of the vibrational levels with atomic oxygen which is the most effective

agent. The rate coefficient[85] for the deactivation of the $v=0$ level by oxygen atom can be expressed as

$$K_{10} = 1.1 \times 10^{-10} \, \text{Exp} \, (-69.9/T_g^{1/3}) \qquad (34)$$

where T_g is in units of eV. The corresponding excitation rate coefficient can be obtained by detailed balance. For the vibrational-vibrational exchange process, the rate coefficient[86] is

$$R_{0,1}^{1,0} = \langle \sigma v \rangle \, \langle P_{01}^{10} \rangle = 3.8 \times 10^{-11} \, (T_g)^{3/2} \qquad (35)$$

Where the exchange probability $\langle P_{01}^{10} \rangle$ is for a harmonic osillator and symmetric resonance exchange. For transition between different vibrational levels with $\Delta v = \pm 1$, harmonic oscillator relations can be utilized. Such a treatment not only will describe appropriately the energy flow between the vibrational and translational modes but also will give the molecular dissociation through the vibrational ladder.

7.1 THERMAL DISSOCIATION AND IONIZATION

In addition to the ionization of air species by electron impact, the air molecules can be dissociated and ionized through thermal collisions. The thermal dissociation rate[87] of N_2 for reaction (36)

$$N_2 + N_2 \rightarrow N + N + N_2 \qquad (36)$$

is $1.90 \times 10^{-9} \, T_g^{-1.6}$ Exp $(-9.76/T_g)$ where T_g is in units of eV and is valid for the temperature range of 0.5 eV to 1.3 eV. The accuracy of this coefficient is within a factor of 3. The thermal dissociation of O_2 with O_2 and N_2 as the collision partner have the following rate coefficients[88] $5.8 \times 10^{-9} \, T_g^{-0.83}$ Exp$(-5.12/T_g)$ and $2.7 \times 10^{-10} \, T_g^{-1.7}$ Exp $(-5.12/T_g)$, respectively, where T_g is in units of eV and their accuracy is within a factor of 3.

8. FINAL REMARKS

A review of major processes and their rate coefficients relevant to the NIL modelling is presented. Schemes for the calculation of the electron energy flow into various modes are also discussed along with the basic air heating processes. The uncertainties in the rates are discussed and recommended values are given. Other chemical processes affecting the NIL modelling will be discussed in a future report along with recommendations for measurements of specific reactions.

27

Table III - Electron impact excitation rate coefficients of

eight ground state vibrational levels of N_2 (cm^3/sec)

T	X_1	X_2	X_3	X_4	X_5	X_6	X_7	X_8
0.1	5.16E-13	3.30E-16	1.45E-16	3.31E-17	1.34E-17	2.48E-18	1.48E-18	4.49E-20*
0.2	1.77E-11	3.15E-12	1.79E-12	8.31E-13	4.69E-13	2.09E-13	1.37E-13	1.87E-14
0.3	1.42E-10	5.97E-11	3.60E-11	2.04E-11	1.31E-11	7.59E-12	5.15E-12	1.01E-12
0.4	4.58E-10	2.42E-10	1.48E-10	9.16E-11	6.27E-11	4.11E-11	2.85E-11	6.70E-12
0.5	9.17E-10	5.32E-10	3.27E-10	2.12E-10	1.51E-10	1.05E-10	7.44E-11	1.95E-11
0.6	1.43E-09	8.68E-10	5.32E-10	3.55E-10	2.50E-10	1.90E-10	1.35E-10	3.79E-11
0.7	1.91E-09	1.20E-09	7.30E-10	4.96E-10	3.71E-10	2.78E-10	2.00E-10	5.90E-11
0.8	2.33E-09	1.49E-09	9.05E-10	6.23E-10	4.73E-10	3.61E-10	2.61E-10	8.01E-11
0.9	2.67E-09	1.73E-09	1.05E-09	7.29E-10	5.60E-10	4.34E-10	3.16E-10	9.98E-11
1.0	2.95E-09	1.92E-09	1.16E-09	8.13E-10	6.31E-10	4.94E-10	3.61E-10	1.17E-10
1.1	3.16E-09	2.07E-09	1.25E-09	8.78E-10	6.87E-10	5.42E-10	3.99E-10	1.31E-10
1.2	3.31E-09	2.18E-09	1.31E-09	9.26E-10	7.29E-10	5.79E-10	4.27E-10	1.43E-10
1.3	3.41E-09	2.26E-09	1.35E-09	9.60E-10	7.50E-10	6.07E-10	4.49E-10	1.52E-10
1.4	3.48E-09	2.31E-09	1.38E-09	9.82E-10	7.81E-10	6.27E-10	4.65E-10	1.59E-10
1.5	3.51E-09	2.34E-09	1.39E-09	9.94E-10	7.94E-10	6.40E-10	4.76E-10	1.64E-10
1.6	3.52E-09	2.35E-09	1.40E-09	9.99E-10	8.01E-10	6.47E-10	4.83E-10	1.68E-10
1.7	3.51E-09	2.35E-09	1.39E-09	9.98E-10	8.02E-10	6.50E-10	4.86E-10	1.71E-10
1.8	3.49E-09	2.33E-09	1.38E-09	9.92E-10	8.00E-10	6.50E-10	4.87E-10	1.72E-10
1.9	3.45E-09	2.31E-09	1.37E-09	9.82E-10	7.94E-10	6.57E-10	4.85E-10	1.72E-10

* 4.49E-20 reads 4.49 x 10^{-20}

TABLE III (Continued)

Electron impact excitation rate coefficients of

eight ground state vibrational levels of N_2 (cm^3/sec)

| T	X_1	X_2	X_3	X_4	X_5	X_6	X_7	X_8
2.0	3.41E-09	2.29E-09	1.35E-09	9.70E-10	7.85E-10	6.42E-10	4.82E-10	1.72E-10
2.1	3.36E-09	2.25E-09	1.32E-09	9.55E-10	7.76E-10	6.35E-10	4.78E-10	1.72E-10
2.2	3.30E-09	2.22E-09	1.30E-09	9.40E-10	7.65E-10	6.26E-10	4.72E-10	1.70E-10
2.3	3.24E-09	2.18E-09	1.28E-09	9.23E-10	7.52E-10	6.17E-10	4.65E-10	1.68E-10
2.4	3.18E-09	2.14E-09	1.25E-09	9.05E-10	7.39E-10	6.07E-10	4.58E-10	1.66E-10
2.5	3.11E-09	2.09E-09	1.22E-09	8.83E-10	7.26E-10	5.97E-10	4.51E-10	1.64E-10
2.6	3.05E-09	2.05E-09	1.20E-09	8.69E-10	7.11E-10	5.86E-10	4.43E-10	1.62E-10
2.7	2.98E-09	2.01E-09	1.17E-09	8.50E-10	7.09E-10	5.74E-10	4.35E-10	1.59E-10
2.8	2.92E-09	1.96E-09	1.15E-09	8.32E-10	6.83E-10	5.63E-10	4.27E-10	1.57E-10
2.9	2.85E-09	1.92E-09	1.12E-09	8.14E-10	6.68E-10	5.52E-10	4.18E-10	1.37E-10
3.0	2.79E-09	1.88E-09	1.09E-09	7.95E-10	6.54E-10	5.40E-10	4.10E-10	1.51E-10
3.1	2.73E-09	1.84E-09	1.07E-09	7.78E-10	6.40E-10	5.29E-10	4.02E-10	1.48E-10
3.2	2.67E-09	1.80E-09	1.04E-09	7.60E-10	6.25E-10	5.18E-10	3.93E-10	1.45E-10
3.3	2.61E-09	1.76E-09	1.02E-09	7.43E-10	6.12E-10	5.07E-10	3.85E-10	1.43E-10
3.4	2.55E-09	1.72E-09	9.98E-10	7.25E-10	5.99E-10	4.96E-10	3.77E-10	1.40E-10
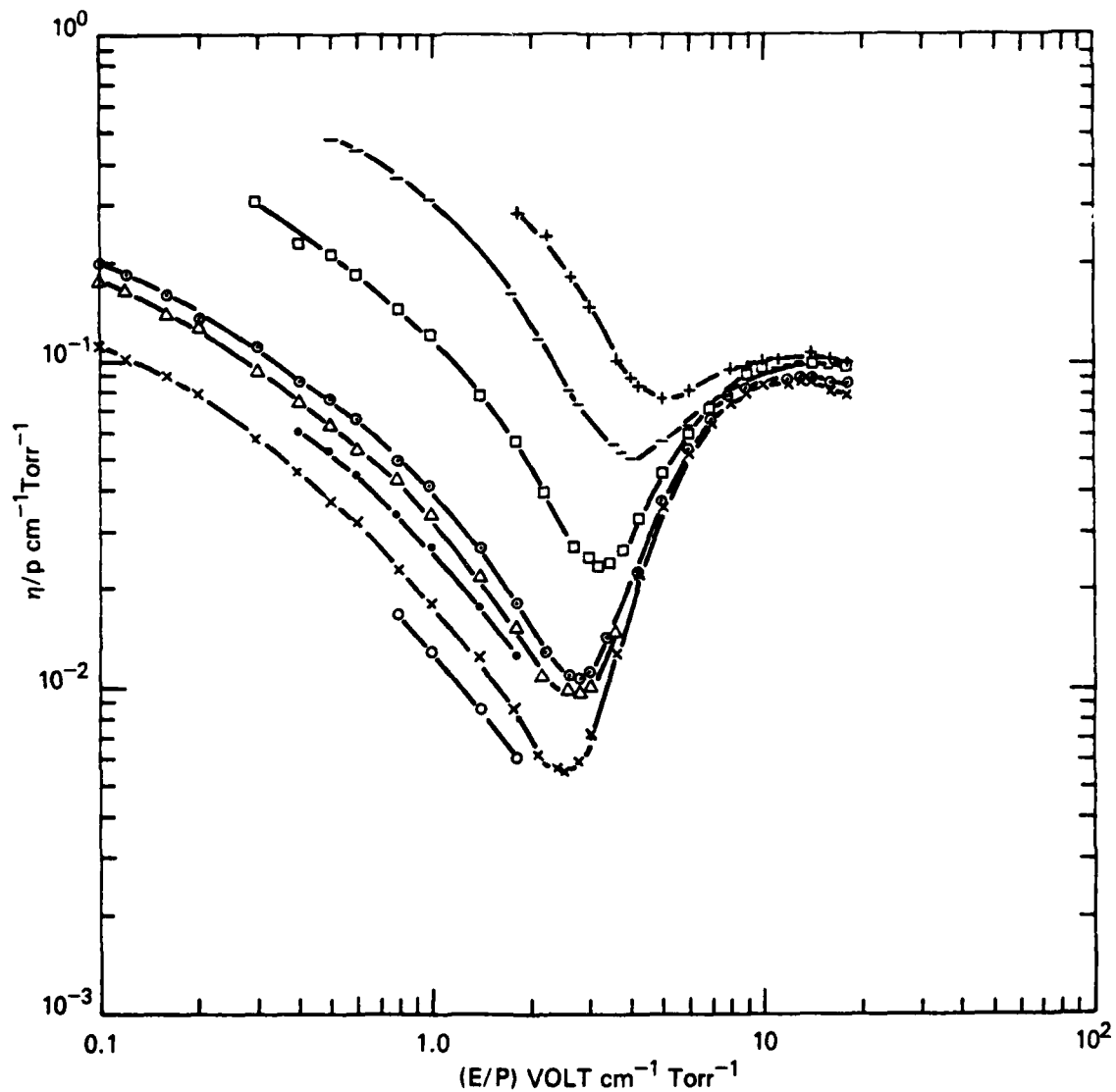
Fig. 1. The attachment coefficient per unit length in O_2 as a function of E/p for various pressures in Torrs (o,o = 14.9, xx = 21.0, •• = 29.7, $\triangle\triangle$ = 36.4, $\theta\theta$ = 44, ___ = 132, -- = 440 and ++ = 880.
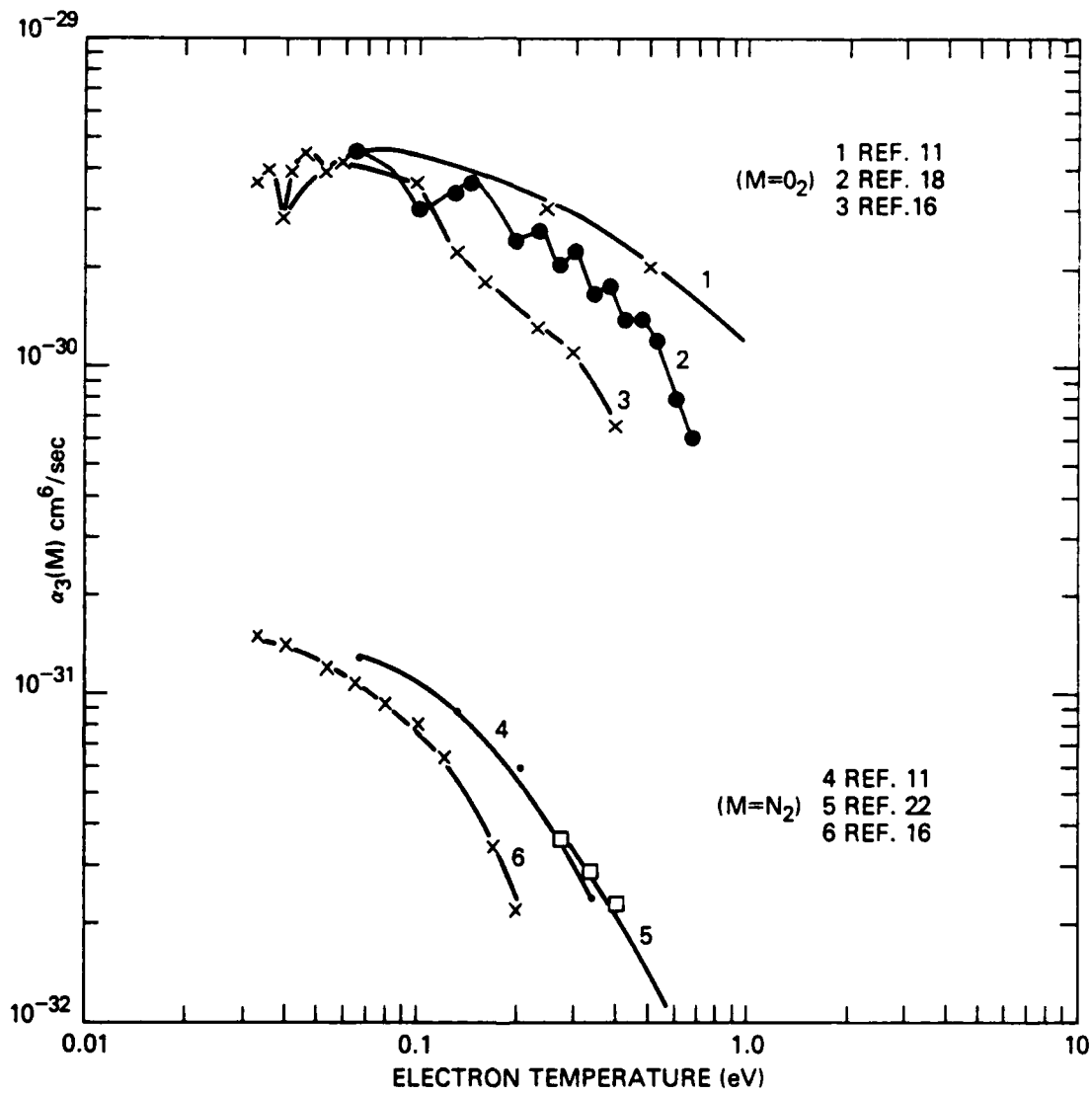
Fig. 2. The attachment rate coefficient with M = O_2 and N_2 as a function of the electron temperature.
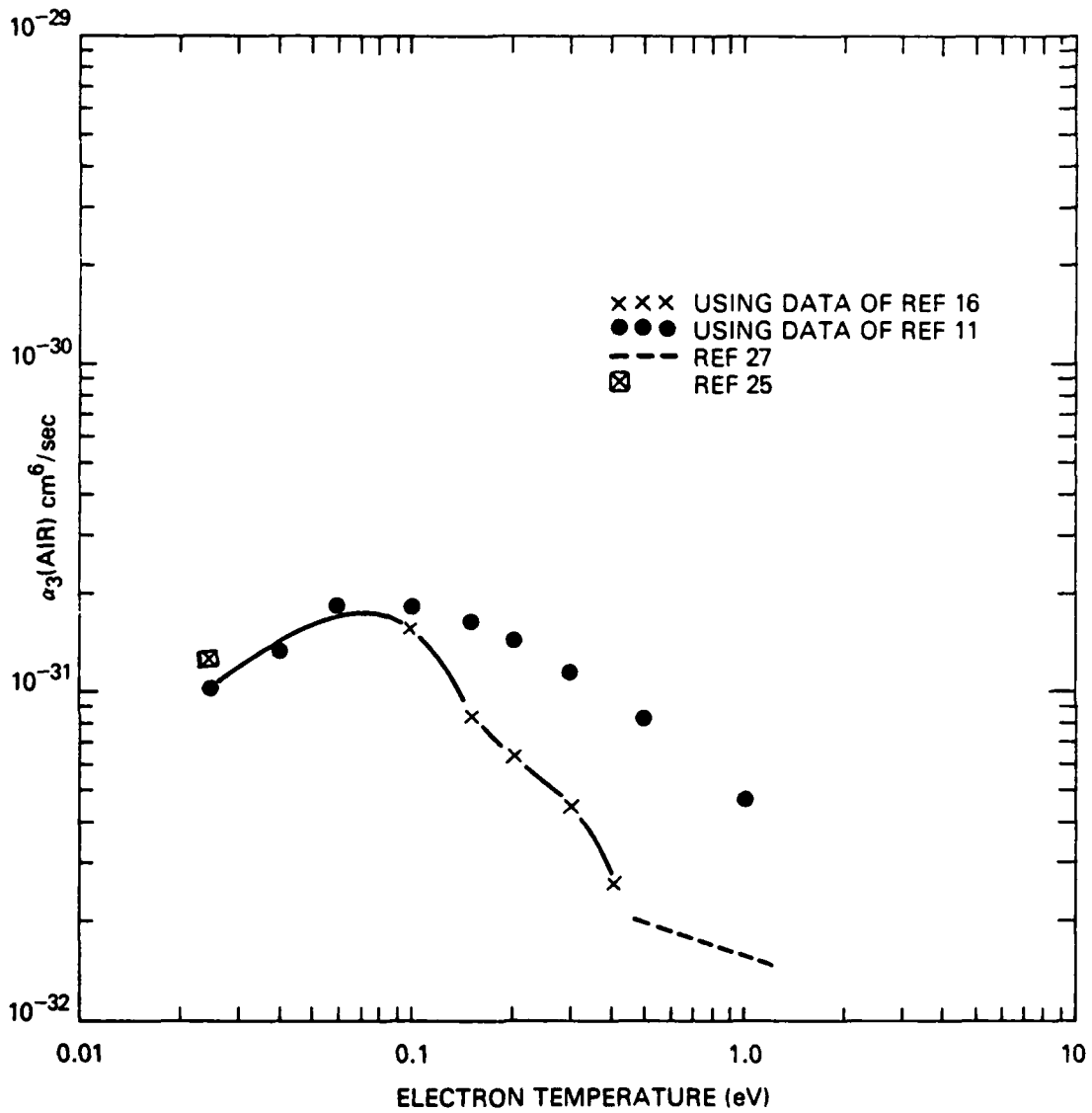
31

Fig. 3. The attachment rate coefficient in dry air as a function of the electron temperature.
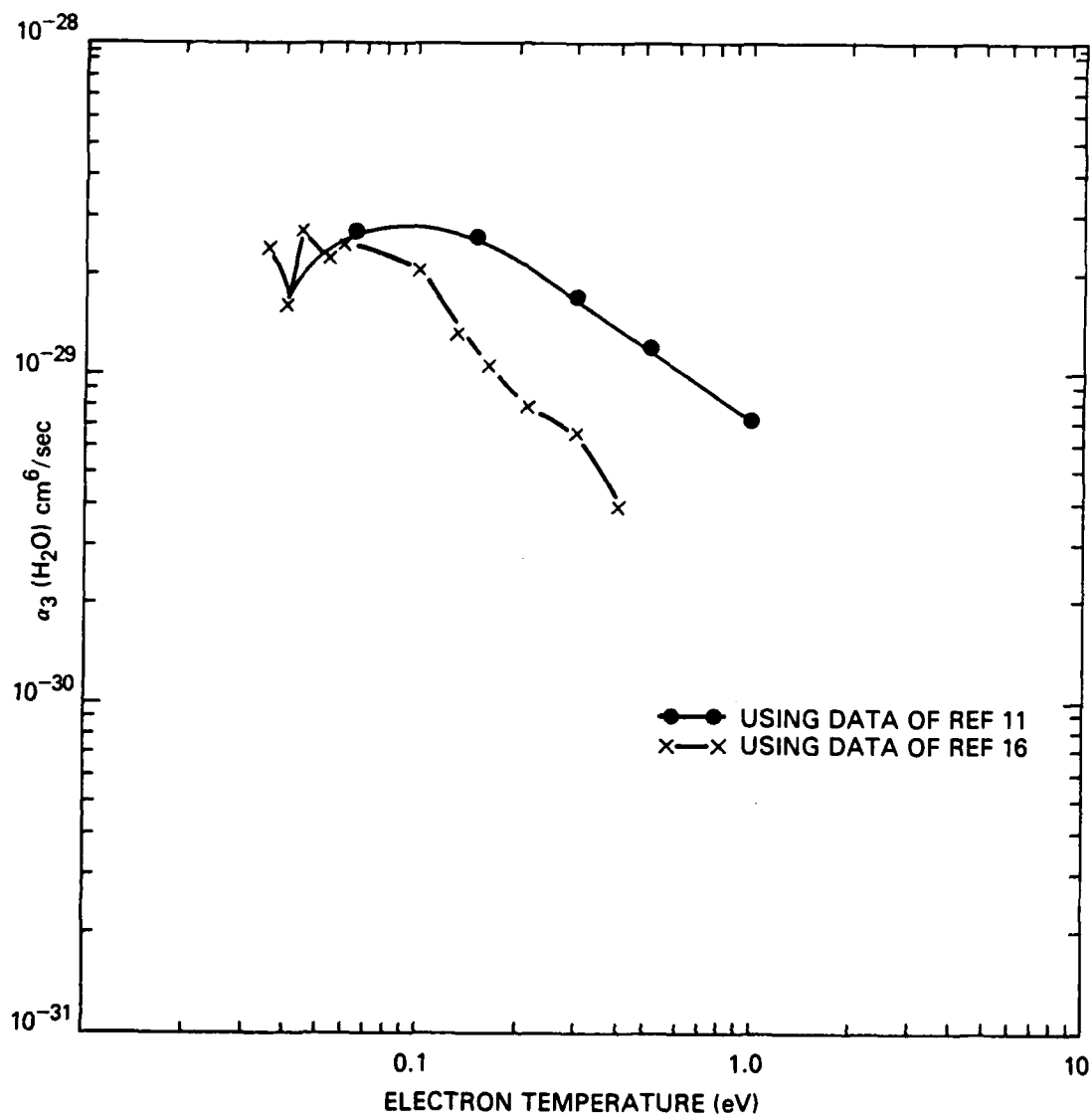
Fig. 4. The attachment rate coefficient with M = H_2O as a function of the electron temperature.
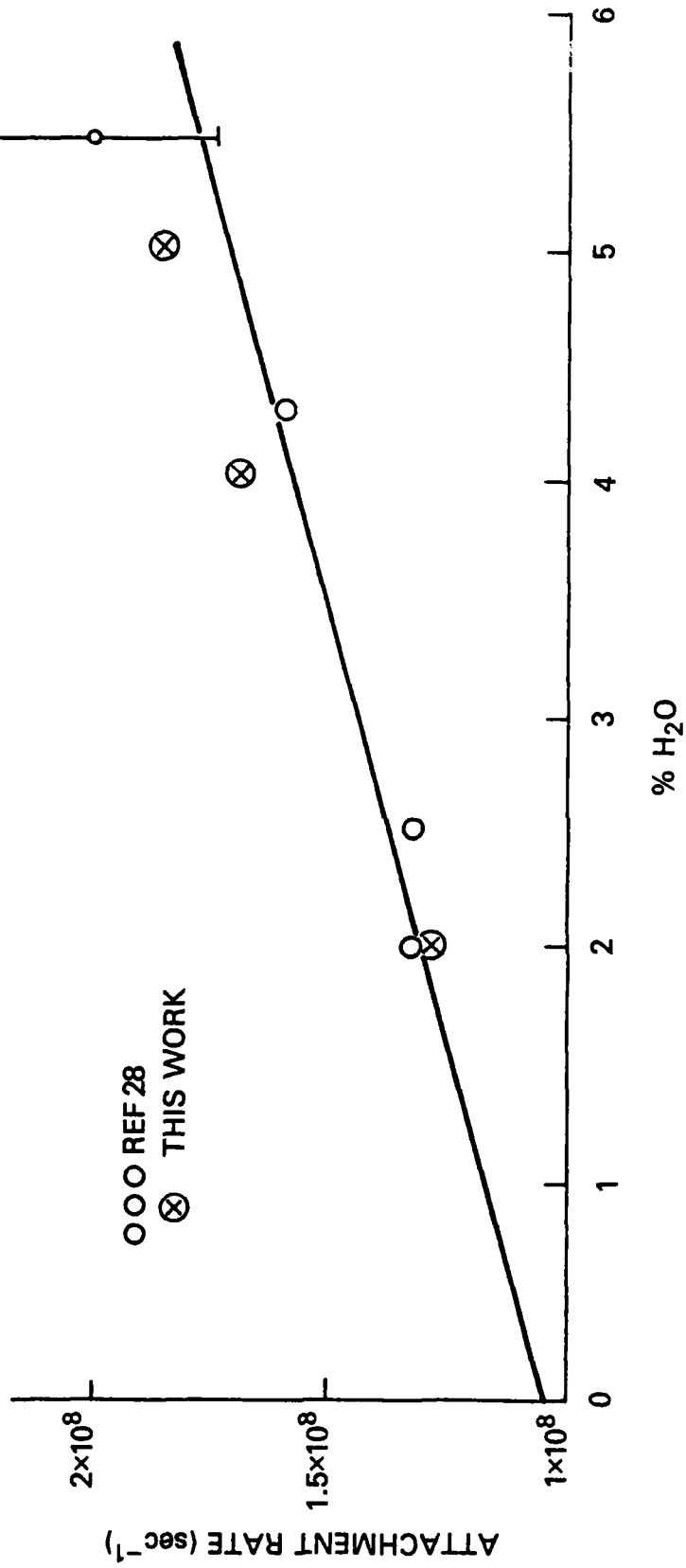
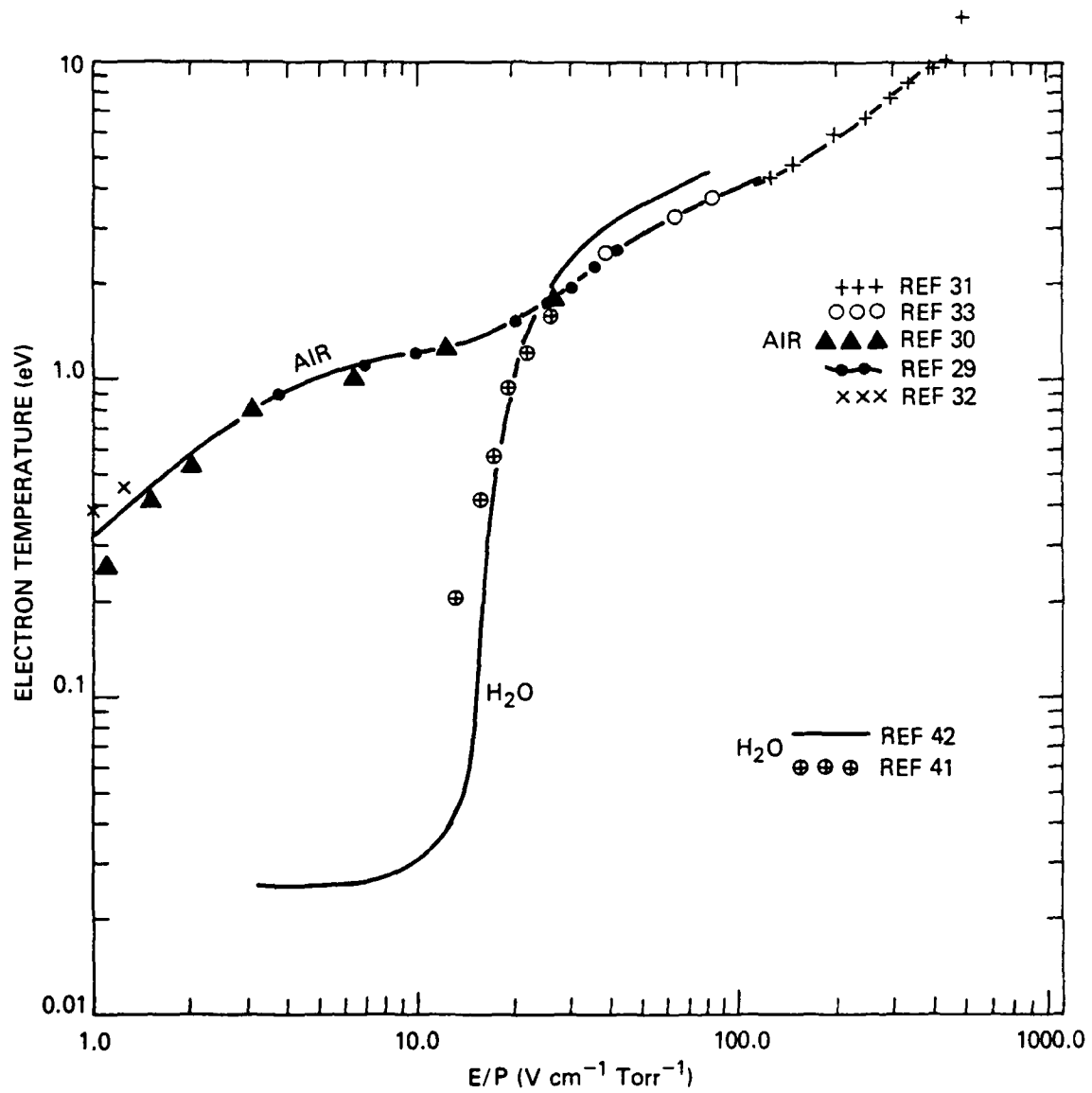Fig. 5.   The attachment rate in air for various concentrations of H_2O.

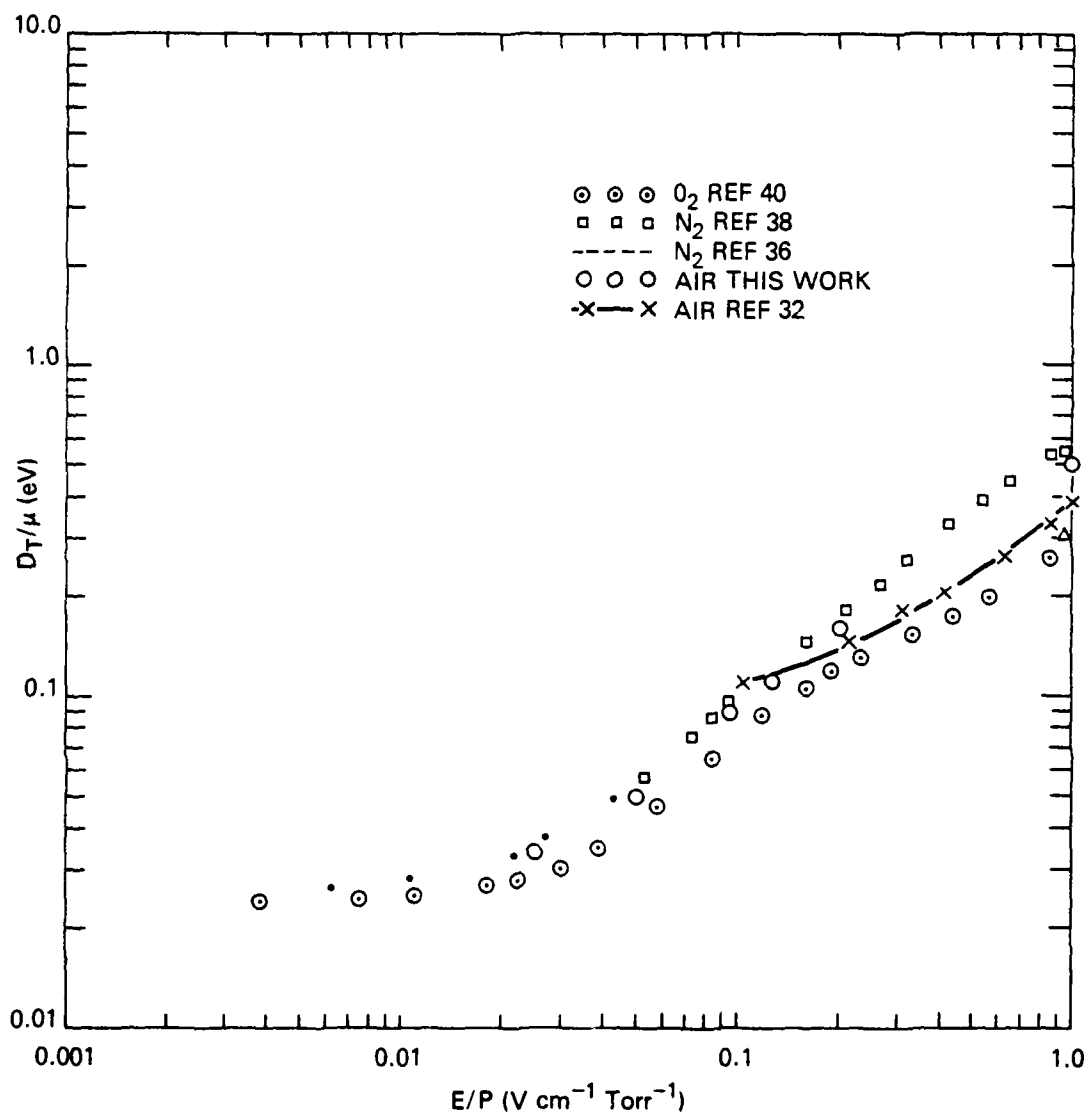Fig. 6a. The electron temperature in air and H_2O as a function of E/p.

Fig. 6b. The electron temperature in N_2, O_2 and air as a function of E/p.

REFERENCES

1. M. A. Uman, D. F. Seacord, G. H. Price and E. T. Pierce, J. Geophys. Res. 77, 1591 (1972).

2. A. D. MacDonald, "Microwave Breakdown in Gases" (Wiley, New York, 1966).

3. C. L. Longmire, R. L. Gardner, J. L. Gilbert and M. H. Frese, Lightning Phenomenology Notes, Note 4, A Physical Model of Nuclear Lightning (March 1982) Mission Research Corporation.

4. D. A. Reib "Uncertainties in the Calculations of High Altitude EMP", AFWL-TR-79-205 Air Force Weapons Laboratory, Kirtland Air Force Base, NM (1981). (AD-B056 361L)

5. M. Scheibe "The Increased Attachment Due to Ionizations Induced Smog in EMP Environments" DNA 5077F, Defense Nuclear Agency (1979). (AD A087-850)

6. M. K. Grover and F. R. Gilmore "A Review of Data for Electron Mobility, Energy, and Attachment Relevant to EMP Air Chemistry" DNA 5457T, Defense Nuclear Agency (1980). (AD A098847)

7. D. Rapp and D. D. Briglia, J. Chem. Phys. 43, 1480 (1965).

8. S. Slinker and A. W. Ali, "Electron Excitation and Ionization Rate Coefficients for N_2, O_2, NO, N and O", NRL Memo Report 4756 (1982). (ADA110988)

9. A. V. Phelps, Canad, J. Chem. 47, 1783 (1969) and references therein.

10. A. V. Phelps, Chapter 17, "DNA Reaction Rate Handbook," DNA 1948H, Bortner and Baurer, Eds., DASIAC, DOD Nuclear Information and Analysis Center GE-Tempo, Santa Barbara, CA (1972). (AD-821 457L)

11. L. M. Chanin, A. V. Phelps and M. A. Biondi, Phys. Rev. 128, 219 (1962).

12. J. L. Pack and A. V. Phelps, J. Chem. Phys. 44, 1870 (1966).

13. H. Shimamori and Y. Hatano, Chem. Phys. 12, 439 (1976).

14. H. Shimamori and Y. Hatano, Chem. Phys. 21, 187 (1977).

15. F. K. Truby, Phys. Rev. A 6, 671 (1972).

16. D. L. McCorkle, L. G. Christophorou and V. E. Anderson, J. Phys. B. Atom. Mol. Phys. 5, 1211 (1972).

17. M. N. Hirsh, P. N. Eisner and J. A. Slevin, Phys. Rev. 178, 175 (1969).

18. D. Spence and G. J. Schulz, Phys. Rev. A, 5, 724 (1972).

19. R. Grünberg, Z. Naturfrosh, 24a, 1039 (1969).

20. See e.g. J. Dutton, J. Phys. Chem. Ref. Data 4, 577 (1975).

21. F. Bloch and N. E. Bradbury, Phys. Rev. 48, 689 (1935).

22. G. S. Hurst and T. E. Bortner, Phys. Rev. 114, 116 (1959).

23. J. L. Pack and A. V. Phelps, J. Chem. Phys. 45, 4316 (1966).

24. J. A. Stockdale, L. G. Christophorou and G. S. Hurst, J. Chem. Phys 47, 3267 (1967).

25. V. N. Kapinos, Yu. A. Medvedev, N. N. Morozov and B. M. Stepanov, Soviet Phys. Tech. Phys. 19, 1507 (1975).

26. M. L. Price and V. A. Van Lint "Measurement of Electron Attachment and Mobility in Dry and Wet Air" MRC/SD-R-31, DNA (1978), Mission Research Corp., (AD-A071 333)

27. B. I. Schneider and C. A. Brau, J. Phys B, Atom. Mol. Phys. 15, 1601 (1982).

28. V. Van Lint and M. Price, Mission Research Corporation Report July 17 (1979) DNA Contract DNA 001-78-C-0141.

29. J. A. Rees and R. L. Jory, Aust. J. Phys. 17, 307 (1964).

30. C. Raja Rao and G. R. Govinda Raju, J. Phys. D 4, 769 (1971).

31. C. S. Lakshminarasimha and J. Lucas, J. Phys D 10,313 (1977).

32. R. W. Crompton, L. G. H. Huxley and D. J. Sutton, Proc. R. Soc. London A218 507 (1953).

33. V. N. Maller, M. S. Naidu, Indian J. Pure. Appl. Phys. 14, 733 (1976).

34. J. W. Gallagher, E C. Beaty, J. Dutton and L. C. Pitchford, JILA Information Center Report #22, University of Colorado, Boulder, CO. 1982.

35. L. S. Frost and A. V. Phelps, Phys. Rev. 127, 1621 (1962).

36. R. W. Crompton and M. T. Elford, Proceedings of the Int. Conf. Ionization Phenomena in Gases, Paris (1963). V. 1, p. 337.

37. L. W. Cochran and D. W. Forester, Phys. Rev. 126, 1785 (1962).

38. R. L. Jory, Aust. J. Phys. 18, 237 (1965).

39. J. J. Lowke and J. H. Parker, Jr., Phys. Rev. 181, 302 (1969).

40. R. D. Hake, Jr., and A. V. Phelps, Phys. Rev. 158, 70 (1967).

41. J. E. Parr and J. L. Moruzzi, J. Phys. D, 5, 514 (1972).

42. J. F. Wilson, F. J. Davis, D. R. Nelson, and R. N. Compton, J. Chem. Phys. 62, 4204 (1975).

43. J. T. Moseley, R. E. Olson and J. R. Peterson "Case Studies in Atomic Physics" 5, 1, (1976) North-Holland (New York), and References therein.

44. D. Smith, N. G. Adams and M. J. Church, Planet Space Science 24, 697 (1976).

45. D. Smith and M. J. Church, Planet Space Sci. 25, 433 (1977).

46. P. M. Eisner and M. N. Hirsh, Phys.Rev. Lett. 26 87 (1971).

47. J. C. Ulwick, "Proc. COSPAR Symp. on Solar Particle Event of Nov. 1969" AFCRL-TR-72-0474, Special Report #144,511 AFCRL, Bedford, MA (1972). (AD-763081)

48. R. E. Olson, J. Chem. Phys, 56, 2979 (1972).

49. D. R. Bates, Advances in Atomic and Molecular Physics 15, Bates and Bederson, Eds., Academic Press (New York) (1979). p. 235-262.

50. S. McGowan, Can. J. Phys. 45, 439 (1967).

51. J. Sayers, Proc. Roy. Soc. (London) Ser. A 169, 83 (1938).

52. J. G. Chervenak and V. A. J. Van Lint, Private communication to A. Phelps (1980).

53. See e.g., E. W. McDaniel, "Collision Phenomena in Ionized Gases", Wiley, New York (1973).

54. B. H. Mahan, Adv. Chem. Phys. Vol. 23 Wiley, New York (1973). p. 1-40.

55. A. Phelps, JILA, University of Colorado, private communications (1983).

56. F. H. Sanders, Phys. Rev. 44, 1020 (1933).

57. K. Masch, see e.g. Reference 20.

58. C. Raja Rao and G. R. Govinda Raju, J. Phys. D4, 494 (1971)

59. J. L. Moruzzi and D. A. Price, J. Phys. D7, 1434 (1974)

60. A. W. Ali, "The Electron Avalanche Ionization of Air and a Simple Air Chemistry Model", NRL Memo Report 4794 (1982). (AD-A113501)

61. H. Ryzko, Proc. Phys. Soc (London) 85, 1283 (1965).

62. L. Frommhold, Fortschr. Physik 12, 597 (1964).

63. R. N. Varney, Phys. Rev. 89, 708 (1953).

64. R. N. Varney, J. Chem. Phys. 31, 1314 (1959).

65. R. N. Varney, J. Geophy. Res. 72, 5578 (1967).

66. R. N. Varney, Phys. Rev. 174, 165 (1968).

67. P. Warneck, J. Chem. Phys. $\underline{46}$, 502 (1967).

68. A. Good, D. A. Durden and P. Kebarle, J. Chem. Phys. $\underline{53}$, 4723 (1970).

69. J. L. Payzant and P. Kebarle, J. Chem. Phys. $\underline{53}$, 4723 (1970).

70. J. L. McCrumb and P. Warneck, J. Chem. Phys. $\underline{66}$, 5416 (1977).

71. S. Dheandhanoo, R. Johnsen and M. A. Biondi, $35\underline{th}$ Gaseous Electronics Conf., U. of Texas at Dallas Oct. 19 (1982).

72. A. W. Ali, "On Electron Beam Ionization of Air and Chemical Reactions for Disturbed Air Deionization", NRL Memo Report 4619 (1981).

73. J. T. Mosely, R. M. Snuggs, D. W. Martin and E. W. McDaniel, Phys. Rev. $\underline{178}$, 240 (1969).

74. C. J. Howard, V. M. Bierbaum, H. W. Rundle and F. Kaufman, J. Chem. Phys. $\underline{57}$, 3491 (1972).

75. D. J. Payzant, A. J. Cunningham and P. Kabarle, J. Chem. Phys. $\underline{59}$, 5615 (1973).

76. D. A. Durden, P. Kebarle and A. Good, J. Chem. Phys. $\underline{50}$, 805 (1969).

77. D. L. Albritton, Atomic Data and Nuclear Tables $\underline{22}$, 1 (1978).

78. See e.g. A. W. Ali, "The Fundamentals of the 3914Å and 3371Å Emissions for N_2 and Air Plasma Diagnostics", NRL Memo Report 4927 (1982).

79. E. C. Zipf and R. W. McLaughlin, Planet. Space Sci. $\underline{26}$, 449 (1978).

80. A. W. Ali and S. Slinker, $16\underline{th}$ Int. Conf. Phenom. Ioniz. Gases, Botticher, Wenke and Schulz-Gulde Eds., Volume 4, 596, Dusseldorf (1983).

81. A. W. Ali and A. D. Anderson, "Low Energy Electron Impact Rate Coefficients for Some Atmospheric Species", NRL Report 7432 (1972).

82. G. J. Schulz, Phys. Rev. $\underline{135}$, A988 (1964) and References therein.

83. H. Ehrhardt and R. Willman, Zeits, Phys. 204, 462 (1967).

84. D. Spence, J. L. Mauer and G. J. Schulz, J. Chem. Phys. $\underline{57}$, 5516 (1972).

85. R. J. McNeal, M. E. Whitson and G. R. Cook, J. Geophys. Res. $\underline{79}$, 1527 (1974).

86. A. W. Ali, Unpublished.

87. D. L. Baulch, D. D. Drysdale, D. G. Horne and A. C. Lloyd "Evaluated Kinetic Data for High Temperature Reactions", Vol. 1, CRC Press (1972).

88. M. H. Bortner, NBS Technical Note 484 (1969).

DISTRIBUTION LIST

Director
Defense Advanced Research Projects Agency
Architect Building
1400 Wilson Blvd.
Arlington, VA 22209
    ATTN: Nuclear Monitoring Research
             Strategic Tech Office

Director
Defense Nuclear Agency
Washington, DC 20305
    ATTN: STVL
             TITL   (4 copies)
             DDST
             RAAE   (3 copies)

Commander
Field Command
Defense Nuclear Agency
Kirtland, AFB, NM 87115
    ATTN: FCPR

Defense Technical Information Center
Cameron Station
5010 Duke Street
Alexandria, VA 22314 (2 copies)

Commander/Director
Atmospheric Sciences Laboratory
U.S. Army Electronics Command
White Sands Missile Range, NM 88002
    ATTN: DELAS-EO F. Niles

Director
U.S. Army Ballistic Research Laboratory
Aberdeen Proving Ground, MD 21005
    ATTN: Tech Library

41

Naval Research Laboratory
Washington, D.C. 20375
    ATTN: Code 4700 S. L. Ossakow (26 copies)
               Code 4701 I. Vitkovitsky
               Code 4780 J. Huba
               Code 7500
               Code 4763 J. R. Grieg
               Code 4763 R. Fernsler
               Code 2628   (20 copies)
               Code 4700.1 A. W. Ali   (30 copies)

Office of Naval Research
Arlington, VA 22217
    ATTN: Code 465
               Code 461
               Code 402
               Code 420
               Code 421

Air Force Geophysics Laboratory
Hanscom AFB, MA 01731
    ATTN: OPR Harold Gardner
               LKB Kenneth S. W. Champion
               OPR Alva T. Stair
               PHD Jurgen Buchau
               PHD John P. Mullen

Berkeley Research Associates, Inc.
P. O. Box 983
Berkeley, CA 94701
    ATTN: J. Workman
               C. Prettie
               S. Brecht

JAYCOR
11011 Torreyana Road
P. O. Box 85154
San Diego, CA 92138
    ATTN: J. L. Sperling

JAYCOR
P. O. Box 30281
Santa Barbara, CA 93130
    ATTN: W. A. Radasky

Kaman Tempo-Center for Advanced Studies
816 State Street
P.O. Drawer QQ
Santa Barbara, CA 93102
    ATTN: DASIAC
               Warren S. Knapp
               William McNamara
               B. Gambill

Lockheed Missiles & Space Co., Inc.
3251 Hanover Street
Palo Alto, CA 94304
    ATTN: Martin Walt Dept. 52-12
               W. L. Imhof Dept. 52-12
               Richard G. Johnson Dept 52-12
               J. B. Cladis Dept 52-12

Los Alamos National Laboratory
Mail Station - E-531
P. O. Box 1663
Los Alamos, NM 87545
    ATTN: J. D. Colvin

Mission Research Corporation
735 State Street
Santa Barbara, CA 93101
    ATTN: M. Scheibe
               Conrad L. Longmire

Mission Research Corporation
1720 Randolph Road, S.E.
Albuquerque, NM 87106
    ATN: L. Wright

Pacific-Sierra Research Corp
12340 Santa Monica Blvd.
Los Angeles, CA 90025
    ATTN: E. C. Field, Jr.

Photometrics, Inc.
4 Arrow Drive
Woburn, MA 01801
    ATTN: Irving L. Kofsky

R & D Associates
P. O. Box 9695
Marina Del Rey, CA 90291
    ATTN: Forest Gilmore
               Robert F. Lelevier

The Rand Corporation
1700 Main Street
Santa Monica, CA 90406
    ATTN: Cullen Crain
               Ed Bedrozian

Science Applications, Inc.
1150 Prospect Plaza
La Jolla, CA 92037
    ATTN: Daniel A. Hamlin

SRI International
333 Ravenswood Avenue
Menlo Park, CA 94025
    ATTN: Walter G. Chesnut

END

FILMED

8